Chapter 5

Mooring Integrity Management: Novel Approaches Towards *In Situ* Monitoring

Ángela Angulo, Graham Edwards, Slim Soua and Tat-Hean Gan

Additional information is available at the end of the chapter

http://dx.doi.org/10.5772/intechopen.68386

Abstract

The recent dramatic fluctuations in oil and gas prices are forcing operators to look at radically new ways of maintaining the integrity of their structures. Moreover, the life of old structures has to be extended. This includes the replacement of expensive periodic in-service inspections with cost-efficient structural health monitoring (SHM) with permanently installed sensors. Mooring chains for floating offshore installations, typically designed for a 25-year service life, are loaded in fatigue in a seawater environment. There is no industry consensus on failure mechanisms or even defect initiation that mooring chains may incur. Moorings are safety-critical areas, which by their nature are hazardous to inspect. Close visual inspection in the turret is usually too hazardous for divers, yet is not possible with remotely operated vehicles (ROVs), because of limited access. Conventional non-destructive techniques (NDTs) are used to carry out inspections of mooring chains in the turret of floating production storage and offloading (FPSO) units. Although successful at detecting and assessing the fatigue cracks, the hazardous nature of the operation calls for remote techniques that can be applied continuously to identify damage initiation and progress. Appropriate replacement plans must enhance current strategies by implementing real-time data retrofit.

Keywords: mooring chain, structural integrity, structural health monitoring, acoustic emission, guided wave, crack growth

1. Introduction

As offshore exploration and production goes further afield and into deeper waters, more offshore operations, e.g. oil and gas operations [1], are conducted from floating platforms moored to the seabed by chains. Mooring lines are safety-critical systems on offshore floating and semi-submersible platforms. The lines are often subject to immense environmental and structural forces from currents, waves and hurricanes. Other forces arise from impact with the seabed, abrasion, increased drag by accumulation of marine organisms and salt water corrosion. Failure of one or more of these mooring lines can result in disastrous and economic consequences for safety, the environment and production.

Periodic inspection of chain systems is mandatory [2] for safety and early detection of faults and is usually performed either through:

- an in-air (outside the water) process that necessitates the removal of the chain for inspection at the surface. Although common practice with movable jack-up drilling rigs, for example, it is not possible with fixed production systems except by taking the system out of production;
- in-water inspection, which is carried out with the chain system *in situ*.

An advantage of in-water inspection being carried out *in situ* is that it is easy to identify which parts of the chain have been in the wear zone, i.e. in the thrash zone and at the fairlead. This is normally more difficult to determine for long lengths of chain inspected on the quayside [3]. However, the most important advantage of in-water inspection is that it can be carried out during the daily production by the facility with minimal stoppage time, hence excluding the need to decommission and the cost to business through lost production.

Currently, the volumetric non-destructive testing (NDT) used in the offshore industrial sector cannot be deployed underwater with the same efficiency without radical adaptation of the technology. In general, current in-water testing techniques have intrinsic issues with probability of detection that are amplified when applied underwater; hence, their use on mooring chains requires highly specialised procedures. This is limited:

- NDT diver-inspections are in general not a favoured option due to health and safety issues, inconsistency of results and an inherent depth limitation and risk, e.g. when checking the thrash zone;
- standalone robotic systems are too large and cumbersome for practical offshore operations. They are not able to inspect the chains in the thrash zone or near the chain fairleads;
- tethered remotely operated vehicles (ROVs) that use both mechanical and optical calliper systems have met with limited success primarily due to their method of deployment on the chain, i.e. they need in-water diver supervision as they have the potential to be knocked out of true positioning and must be recalibrated between successive measurements.

These limitations compromise the capability for early detection of faults, resulting in periodic failures. For example, between 1980 and 2001, the HSE reported [4] that a drilling semi-submersible in the North Sea can expect to experience a mooring failure (anchor dragging, breaking of mooring lines, loss of anchor, winch failures) once every 4.7 operating years, a production semi-submersible once every 9 years and a floating production storage and offloading (FPSO) installation once every 8.8 years, due to failure to detect defects in the chain.

Consequently, reliance must be placed on in-air inspection, resulting in disruption to the daily operations and substantial economic loss for the operating companies, as the production structures require partial/full de-commissioning during the inspection period (**Figure 1**).

On another front, greater demand for energy in Europe [5], depletion of onshore resources and insecurity of supply from geopolitically unstable traditional areas [6], has led to a push for offshore oil and gas exploration in deep water, with substantial interest in marginal production fields. This necessitates floating production systems with massive mooring chain systems to overcome the substantial challenge for economic extraction. The reliability of inspection is dictated by three important factors [7] as follows:

i. the responsible operators must specify their requirements very clearly in terms of the regions to be inspected and the types of flaws or damage mechanism present (any decommissioning would be prohibitively expensive);

ii. the NDT methods, equipment and personnel must be proven to meet the purpose of the inspection through a suitable qualification process;

iii. the selected NDT process must be implemented thoroughly and mitigate the risk of failure, leading to reduction of scrap, repair, rework and workforce, and increased productivity and safety [8].

Figure 1. From left to right: Example of wear and corrosion on a chain link from the sea-bed touch down zone, in-water inspection showing a studded chain which has lost its stud *in situ*, illustration of marine growth on long-term deployed chain, affecting optical in-water inspection, friction-induced bending.

1.1. Damage mechanisms

The life cycle of a mooring system is in excess of 20 years, and it would normally be designed to withstand '100-year period storm' conditions. A typical floating structure has 14 moorings which can amount to nearly 10 km of chain or hybrid chain and polyester rope (central section). Mooring chains are subjected to cyclical loads and therefore fatigue which can cause a chain to break well below the ultimate strength of the material. These loads are due to the hydrodynamic currents in the water, aerodynamic loads on the pulling weight of the platform, and the local conditions causing the lines to have more or less sag depending on the load direction which can render the chains almost straight with a correspondingly higher horizontal tension component and stiffness, 'freezing' [9], hence fatigue. Microscopic physical damage accumulates with continued cyclic loading until cracks form. Once the crack reaches a critical size, brittle fracture occurs, the chain will break and the mooring will fail. A single mooring line failure may cause the platform to capsize. After multiple mooring failures the platform could drift away, losing control of the well-heads, which without de-pressurising would ultimately cause the risers to rupture catastrophically.

Several field studies have found that wear and tear occur in mooring chains links much sooner than anticipated, i.e. the combined wear and corrosion rate over the years is estimated to be 0.6 mm/year which is 50% higher than the maximum values found in corrosion inspection standards, e.g. API's RP2SK, DnV's OSE301. Loss of section of chain links could be due to corrosion, non-axial friction or even sulphate-reducing bacteria (SRB) that induces pitting corrosion, etc. (**Figure 2**). Consequently, there is an urgent need to either:

- increase the frequency of in-air testing, which would cause disturbance of operations at the platforms and decommissioning at each major inspection;

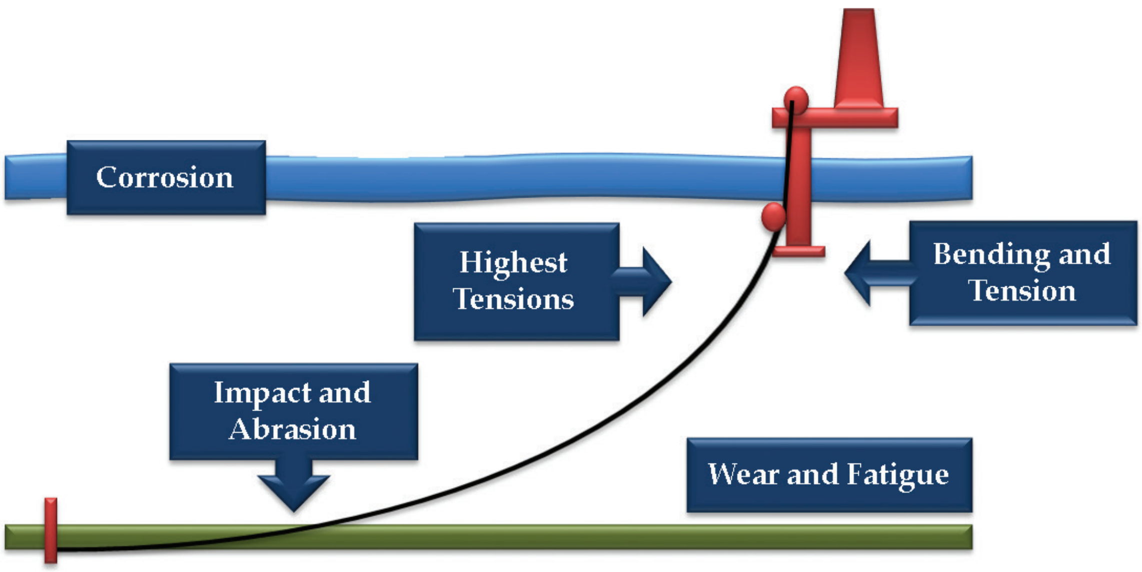

Figure 2. Mooring line degradation and the key areas to inspect.

- or increase the reliability of in-water NDT with a method that can assess progressive wear and tear while the facilities are in operation.

1.2. Innovative character of *in situ* monitoring in relation to the state of the art

Mooring chain life can be significantly reduced, leading to unacceptable risk of catastrophic failure, if early damage is not detected. Chain mounted equipment is available to monitor chain tension and bending, but detection of damage caused by stress concentrations, fatigue, corrosion and fretting or combinations of these is not currently possible. The acoustic emission (AE) technique is capable of detecting cracks in mooring chains and fatigue damage. AE monitoring has shown sensitivity to crack growth during fatigue tests on chains. This chapter will describe the AE technique for detecting fatigue cracks, a procedure for applying the technique, a methodology for incorporating the AE test data with other data in the frame of a holistic approach to integrity management of moorings and a specification for an operational system.

Structural health monitoring (SHM) is the process of implementing a damage detection and characterisation strategy for engineering structures. Damage is defined as changes to the material which adversely affect its performance. The extraction of damage-sensitive features from the very large amount of sensor data normally requires sophisticated statistical analyses.

2. State of the art of inspection methodologies

At present, the state of the art in-water inspection techniques are not reliable; experience has shown that anomalies identified by in-water inspection can only be evaluated with true confidence by in-air inspection.

Specifically, the in-water techniques do not provide early detection of fatigue cracks in the chains and consequently provide little early warning of loss of integrity of moorings. This is mainly due to the inherent difficulties in the logistics of underwater testing and to the inability of the techniques to reach all the areas within the chain links (i.e. contact surfaces between links, marine growth). Several in-water mooring chain NDT systems have been developed with varying levels of success. The main aim for all of them has been to reduce the level of 'human overlooking/presence' in water during the test. These range from a simple diver-deployed manual caliper to prototype stand-alone, ROV-deployed system and a chain climbing robot.

The in-water testing systems mainly deal with two inspection procedures:

- mooring chain system measurement management, i.e. to monitor change in dimensions from the manufacturer's set data as a sign of early development of fatigue cracks and corrosion. This method can be qualitative (provide an indirect measure of damage) or quantitative (provide a measurement);
- mooring chain system integrity, which is used for accurate component condition assessment. This is essential for real-time analysis of progressive defects and can act as an early alarm system.

2.1. Review of current practices

In principle, there are two major stages to the testing of mooring chains:

i. manufacturer's quality control inspection before deployment;

ii. in-service inspection, i.e. for safety and maintenance.

Both types use several known approaches:

- Invasive and destructive testing (IDT). This is usually carried out in-air and either before commissioning of a mooring system (i.e. sample testing) or after clear signs of early damage to the mooring chain (i.e. to establish causes of chain damage during its decommissioning of the chain for future chain design). The main IDT accredited checks are as follows:

  - break testing on at least three links of the same chain, e.g. an applied maximum load for a period of 30 seconds without showing signs of cracking;
  - mechanical testing (tensile and impact).

- Non-destructive testing (NDT) and visual inspection. These do not affect production and can be repeated. Besides visual inspection, the main types of NDT for mooring systems are as follows:

  - Magnetic particle testing (MPT);
  - Penetrant testing;
  - Radiographic testing;
  - Ultrasonic testing.

It is customary to recover the mooring lines part way through their service life for periodic in-air testing, but this has four disadvantages, namely:

(1) the lines may be damaged either during recovery or reinstallation, e.g. losing their studs;

(2) the whole operation is expensive, since the services of anchor handling and possibly heading control tugs will be required for a number of days;

(3) in-air inspection will not necessarily detect all possible cracks and defects;

(4) defects may grow between inspections.

The current situation in the water inspection of mooring lines is accurately reflected in the HSE UK Survey of in-water inspection:

> *'There is an imbalance between the critical nature of mooring systems and the attention HSE receive, i.e. embodied by the frequency and accuracy of real time testing. Currently, there is no in-water technique to check for possible fatigues, cracks and monitor the progressive cases of cracks and defects*

in a real time manner. A new inspection system is needed, which is mostly to be of acoustical nature… It is clearly not appropriate to rely on annual in-water ROVs inspection to check if a mooring line has failed' [4].

From the above discussion, it is clear that an early detection tool for the structural condition of mooring chains would benefit operators to minimize the lost revenue related to unplanned shutdown of offshore oil and gas, wind platforms and other offshore platforms.

2.2. NDT procedures

NDT procedures are key documents. They state which technique is to be used (in NDT terminology, a technique is a specific way of applying an NDT method), the instructions on how it is to be used, including setting up the test equipment and its calibration, the data gathering processes and how the results are to be interpreted. The interpretation must include a methodology for sentencing test signals or indications and distinguishing them from spurious or non-relevant signals. All the NDT methods suffer from a propensity for giving false-calls, where defects are 'called' only to show when examined more closely that nothing is present. Many NDT techniques fall into disrepute when there are too many false calls and for this reason, special effort will be paid to developing procedures that are less prone to error.

The development of any NDT procedure starts with an understanding of the defects being sought. The most important influencing parameters on defect sensitivity in an NDT procedure for chains are the following:

- Type: the defects that are most likely to cause the chain link to fail are cracks emanating from the internal radius and caused by fatigue during fretting movement between the chain links during service and corrosion;
- Location: The internal radius is often the location of very small surface cold laps and cracks created during manufacture of the chain link and these can grow due to fretting between the interlocking chain surfaces. Other defects may be occur in the chain welds as a result of poor quality control during manufacture;
- Size: Chain-links are known with cracks up to half through-wall depth without failure. However, the criticality of cracks in chains is poorly understood. This presents a problem for NDT as there is a limit to the minimum detectable size. Moreover, if the test sensitivity is set too high, the test is likely to be slower and there will be more false-calls.

An example of a recent failure, investigation of a mooring chain link identified fretting in the contact area between the chain links (**Figure 3a**), and the propagation of one crack through the link thickness in a series of fracture faces of increasing diameter (**Figure 3b**).

In the following sections, two well-known SHM techniques have been put forward as an example of novel practices applied to this field: GUW and AE. In order to assess their application to mooring chain monitoring, both modelling and experimental methodologies and results will be described.

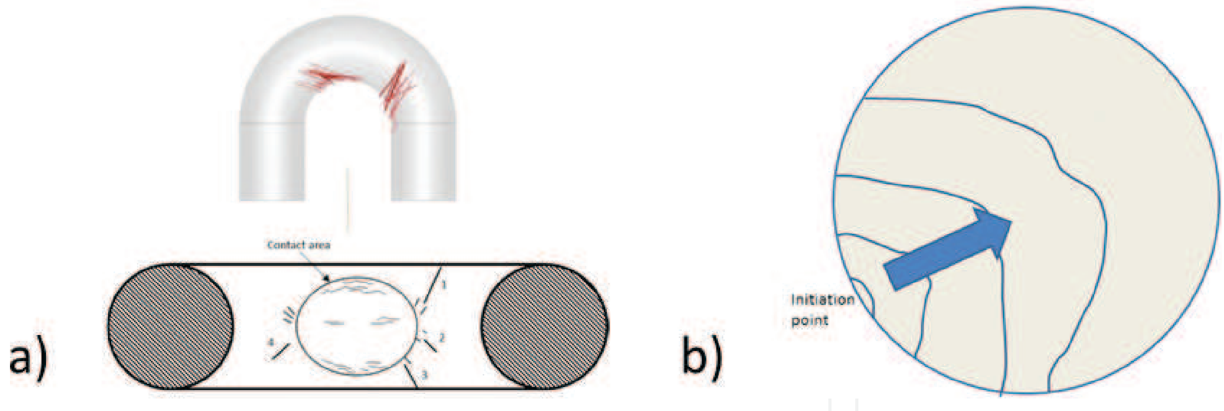

Figure 3. (a) Fretting of contact surfaces between chain links. (b) Fracture surfaces as crack propagates through chain.

3. Guided ultrasonic waves approach

A medium range ultrasonic test (MRUT) has been developed for chains that use guided ultrasonic waves (GUWs). GUWs propagate long distances along elongated objects such as pipes and cylinders, because the multiplying effects of internal reflections from the objects boundaries give rise to waves that are 'guided' and suffer relatively low energy losses. The wave modes are complex however. The so-called 'dispersion curves' (**Figure 4a**) show that as the frequency increases so does the number of wave modes. The additional wave modes increase 'noise' and have the potential to reduce test sensitivity. The high noise due to the presence of multiple GUW modes may be partly compensated with new signal processing algorithms that differentiate the higher-order modes. Alternatively, instead of relying on one ultrasound frequency in the test, the technique might involve a sweep through a range of test frequencies. Some experimental data have already been derived from chains in this way.

GUWs are used in the long-range ultrasonic testing (LRUT) of pipes. In LRUT, the transmitted wave mode from the transducer tool wrapped around the pipe is symmetrical and either longitudinal (L-wave) or torsional (T-wave). However, around chains, a symmetrical wave will become distorted by the chain curvature (**Figure 4b**) to become a flexural (F-wave). The distortion has been studied using numerical models supported by experimentation. Another option is to use Rayleigh waves instead of guided waves. These propagate along the surface only and exist at high frequencies when the frequency-thickness product is beyond a certain limit defined by the thickness of the pipe. However, Rayleigh waves are likely to be strongly affected by surface roughness.

3.1. Finite element modelling

Finite element analysis (FEA) has been used to study the complex GUW propagation around chains and therefore provide a theoretical basis for ultrasound frequency selection for chain links and to aid the optimisation of the inspection technique.

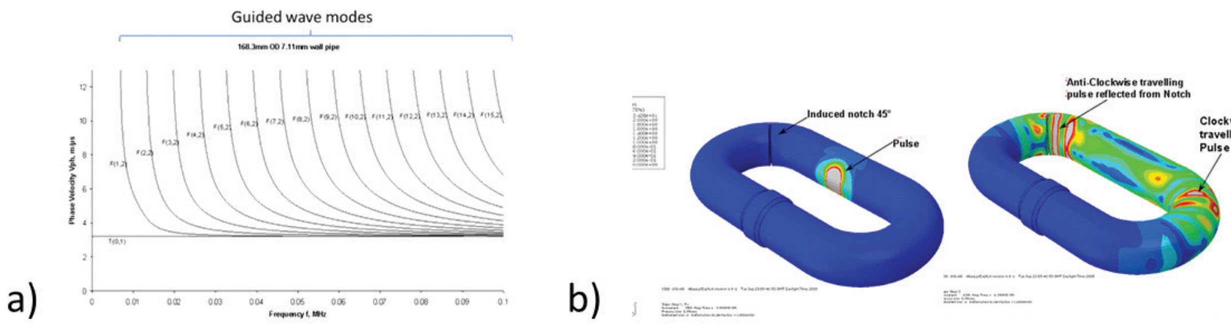

Figure 4. (a) Dispersion curves for a set of GUW modes. (b) Distortion of GUW around a chain.

The modelling work was conducting using the commercially available finite element software, Abaqus. The models were linear elastic and assumed the following material properties for carbon manganese steel.

- Young's modulus = 207 GPa
- Poisson's ratio = 0.3
- Density = 7830 kg/m^3

The finite element mesh was refined such that there were at least eight elements per wavelength for the smallest possible wavelength in the system. The elements used were eight-node linear bricks. In order to investigate the inspection of chain links, a number of models have been generated as follows.

- Natural frequency extraction models to calculate the dispersion characteristics of the straight section of the chain link. This modelling method [10] can be used with most commercial finite element software. It is able to calculate dispersion curves for prismatic structures of any cross section.
- Wave propagation models to calculate the mode conversion that occurs when GUW propagate around the bends in the link.
- Wave propagation analyses of the whole link including the weld at a range of frequencies.

A chain link of diameter 110 mm was used in the analysis.

3.1.1. Modelling results

The natural frequency analyses found that both the T(0,1) and T(0,2) exist at the typical torsional GUW inspection frequencies (20–80 kHz). **Figure 5** shows the displaced shapes and distribution of von-Mises stress in the straight section of the chain link at frequencies of around 45 kHz. The von-Mises stress has been used due to it being independent of the axis system used (e.g. Cartesian or cylindrical). It is proportional to the sound energy. **Figure 5** shows the distribution of von-Mises stress across the cross-section. It can be seen that the amplitude of the T(0,1) wave mode is strongest at the outside surface whereas the T(0,2) wave mode is

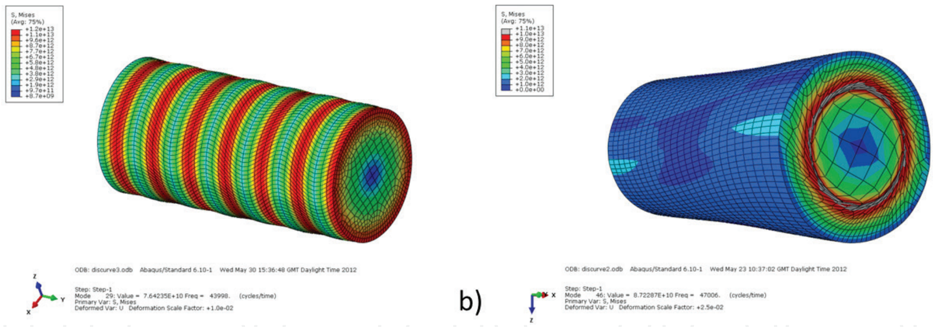

Figure 5. (a) Von-Mises stress distribution of the T(0,1) wave mode at 44 kHz and (b) T(0,2) wave mode at 47 kHz.

subsurface. The distribution of energy may affect the ability to detect flaws in a certain location. The results indicate that T(0,1) would be best for detecting surface breaking flaws. The natural frequency model was also used to extract the displaced shapes of torsional family wave modes.

Next, a wave propagation model was used to understand the behaviour of GUW as they propagate around the bend in the chain link. One bend was modelled and the ends of the model were elongated to prevent end reflections from interfering with the signals received. A single ring of exciters was used so that the pulse would propagate in both directions.

The magnitude of the displacement after excitation of a 10-cycle 40 kHz pulse is shown in **Figure 6**. It can be seen that the signal is no longer axisymmetric after propagation around the bend. This indicates that mode conversion has occurred. Some analysis was carried out to quantify the wave modes present in the signal after propagation around the bend. A mode filtering technique was used to separate the wave modes by circumferential order [12]. Since a torsional excitation was applied, it was assumed that wave modes in the torsional family were present. **Figure 6** shows the amplitudes of the individual wave modes plotted against circumferential order. It can be seen that there is a strong F(1,2) wave mode after passing the bend while T(0,1) wave mode propagates in the other direction along the straight section. The amplitude decreases with increasing circumferential order as would be expected.

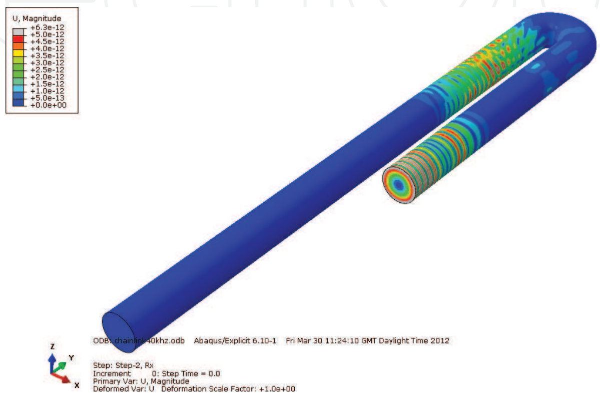

Figure 6. Displacement magnitude after propagation of a 10-cycle 40 kHz pulse around the bend.

Finally, a model of the whole chain link was created and a range of frequencies from 30 to 70 kHz were analysed. Excitation was applied using two rings to match the experimental work, where phasing is used to remove the wave propagating in one direction while reinforcing the wave propagating in the other. The ring spacing was 30 mm and 16 transducers around the circumference were simulated in each ring. The weld was idealised to a triangular shape with a height of 5 mm and a length of 60 mm on the opposite side of the chain from the ring. **Figure 7** shows the von-Mises stress in the chain link just after the input of a 10-cycle 30 kHz pulse. As before, it is clear that significant mode conversion has occurred.

Figure 8 shows the predicted A-scans from each of the models. The mode filtering technique was applied so that the A-scan for individual modes could be assessed. At 30 kHz, the reflections from the weld were distinct and there is relatively little 'noise' in between, whereas at 40 and 60 kHz, the reflections are less clear and the signals caused by the pulses of ultrasound circulating the chain become evident. The algorithm that is used to eliminate signals from pulses 'going the wrong' way through the rings starts to break down for certain wavelengths, and the circulating through-transmission pulses become superimposed on the pulse-echoes. At 50 kHz, there was a lot of noise at the start of the trace. This is likely to be caused by the T(0,2) wave mode. Its cut-off is around 50 kHz and therefore it is only excited at frequencies of 50 kHz and above. However, around its cut-off frequency, it will be highly dispersive which could cause this effect.

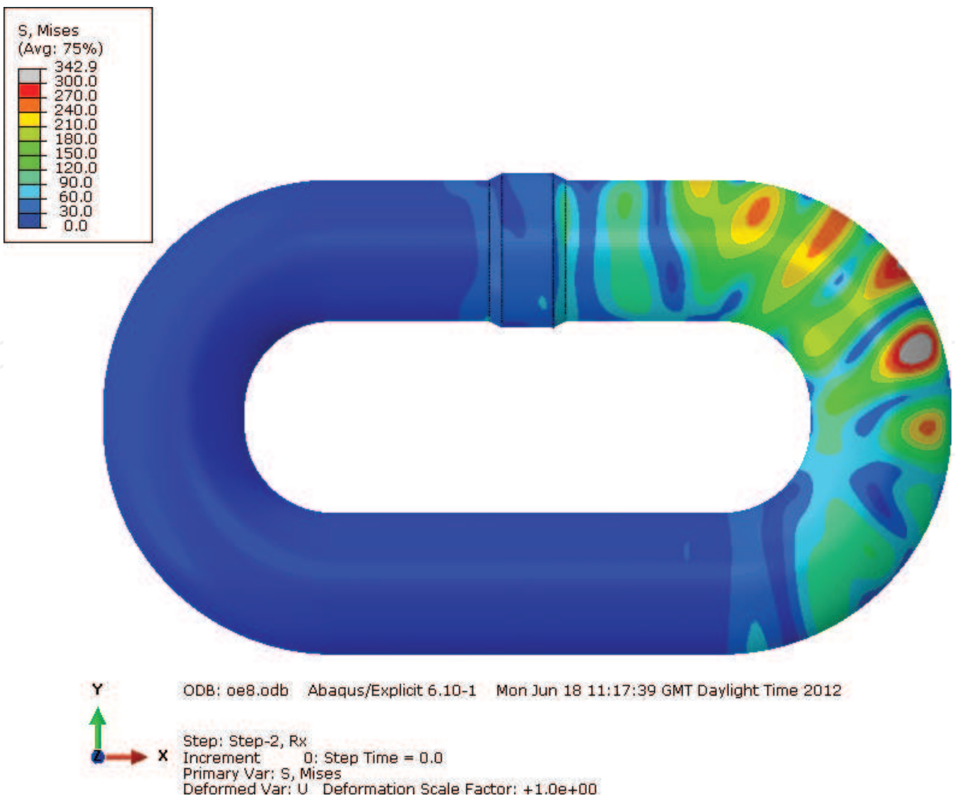

Figure 7. Von-Mises stress distribution in a chain link just after excitation of a 10-cycle 30 kHz pulse.

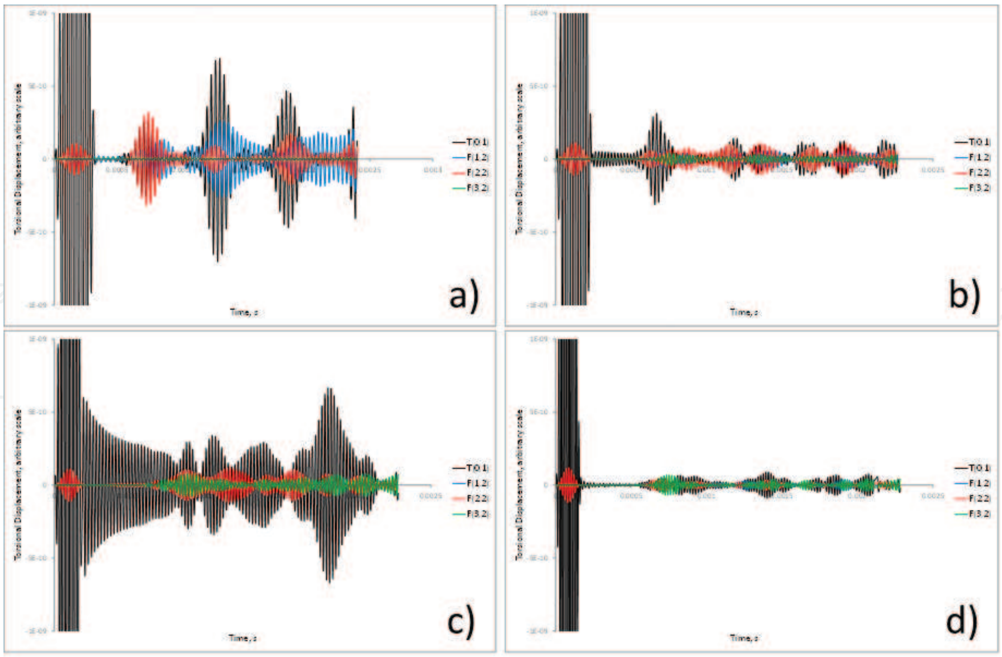

Figure 8. Predicted A-scan of individual wave modes for a: (a) 10-cycle 30 kHz excitation, (b) 10-cycle 40 kHz excitation, (c) 10-cycle 50 kHz excitation and (d) 10.

Finally, the model of the chain link was used to simulate a 50% cross-sectional area flaw for the 10-cycle 30 kHz case. The flaw was approximately 3 mm wide. **Figure 9** shows the layout of the model. **Figure 9** shows the predicted A-scans for individual modes. When compared with **Figure 10** it can be seen that the difference is quite noticeable indicating that detection of the presence of the 50% cross-sectional area of the flaw is possible.

3.2. Methodology and laboratory experiments on chain links

Modelling work was carried out, but under the important proviso that the test procedures used were not 'optimum'. In other words, further on-going work was/is needed on wave

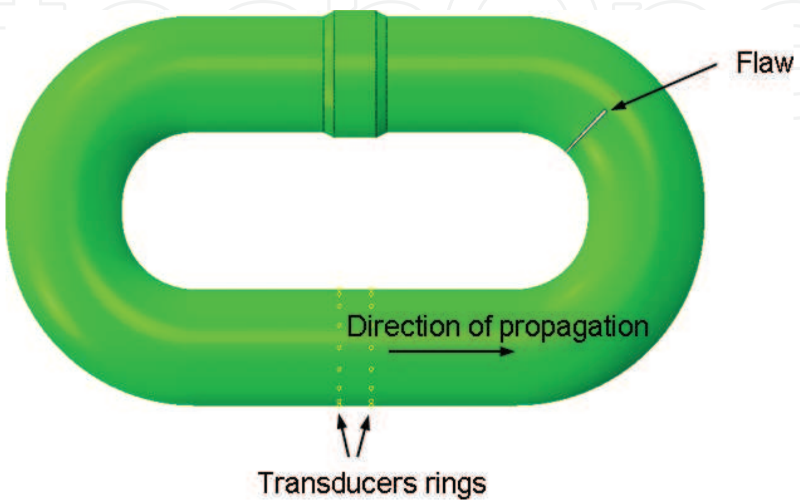

Figure 9. Layout of model of chain link with 50% cross-sectional area loss flaw.

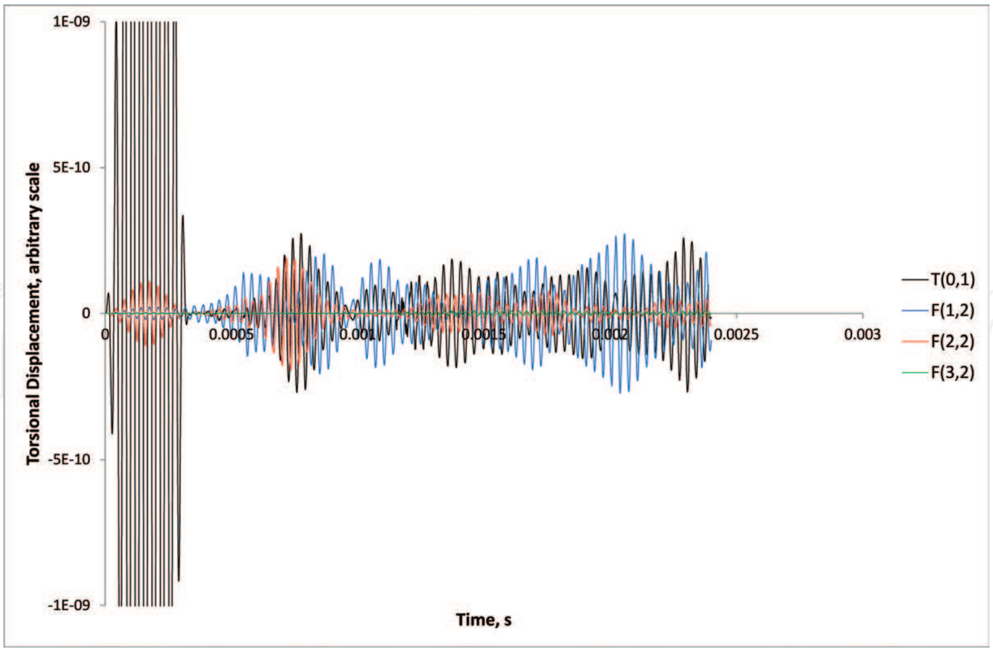

Figure 10. Predicted A-scan of individual wave modes for a 10-cycle 30 kHz excitation in a chain link with a 50% cross-sectional area loss flaw.

propagation in solid cylinders and around bends, selection of ultrasound frequency and pulse length, tool design, etc.

110 mm diameter chains were available for this work. Although this size is at the bottom of the range of chain sizes of interest to the end-users, the availability of the 110 mm diameter 3-m long solid rod on which to calibrate the A-scans was an important advantage at this stage of the study.

Eight chains were tested, two of which contained a defect by way of an EDM slot or a ground notch. The chains varied slightly from 105 to 110 mm diameter. The diameter is the diameter of the solid rod from which the chain link is forged. Once bent into shape it is welded at the ends to complete the whole link. The diameter determines the overall geometry of the chain.

Two slots were carefully placed on one of the 110-mm chain links; one on the intrados and the other on the extrados. On a second 105 mm chain, a notch on the intrados was 'grown' from 5 to 20% through-wall (**Figure 11**).

Figure 11. Aged chain link with slots.

3.2.1. Guided ultrasonic waves equipment and specifications

An important issue is whether the inspection capsule will be able to carry the instrument. There are advantages in keeping the distance between the instrument and the tool as short as possible, because noise is reduced and the signal is less attenuated.

In GUW techniques, the tool design and its performance is critical for the quality of the test results. To propagate symmetrical GUW into a pipe, the collar around the tool must apply equal pressure to all the transducers in a ring or an array.

In the present application, the transducer tool was always placed on the side of the chain opposite from the weld. Tests were performed with the transducer tool on the weld, but there was a drop in performance due to the unevenness of the surface.

The GUW frequencies were swept from 30 to 100 kHz in 5 kHz steps. The T-wave A-scans were collected over a 3-m range from the transducer and converted into ASC files for analysis.

3.2.2. Experimental results

A typical T-wave rectified A-scan is shown in **Figure 12**. It clearly shows multiple echoes from the weld on the opposite side of the chain form the tool.

The data could be grouped to show signal variation with frequency (**Figure 13**).

Closer analyses of the A-scans, however, show them to be divided into bands (see **Figure 14**):

(1) 30–40 kHz where the weld signals are clearly distinguishable;

(2) 50–60 kHz where a signal appears between the positions of the previous weld signals;

(3) 70–80 kHz where the weld signals are again clearly resolved;

(4) 95–100 kHz where signals cannot be distinguished from the noise.

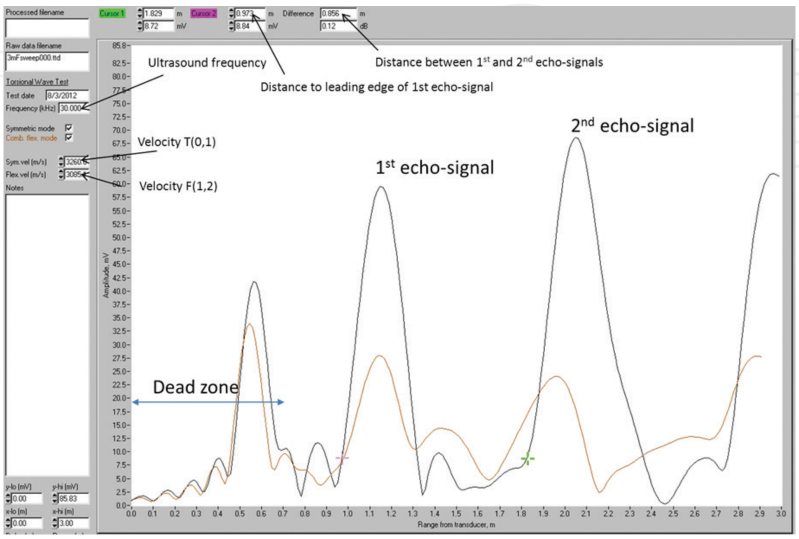

Figure 12. 30 kHz T-wave A-scan from 110 mm chain link.

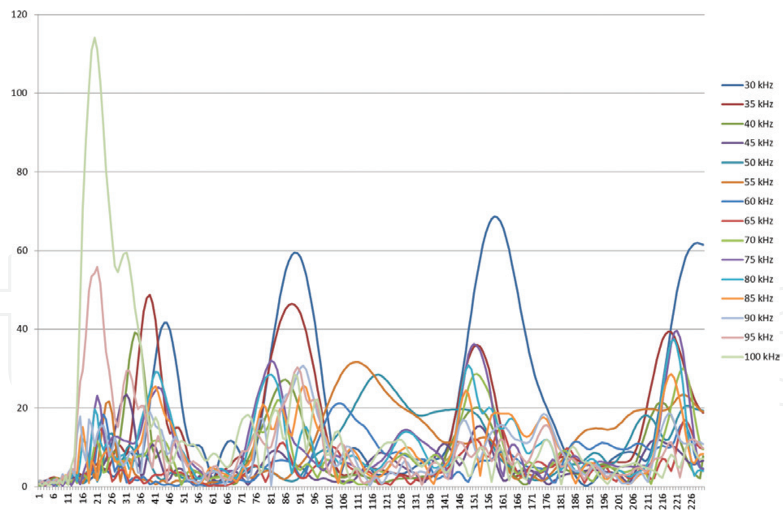

Figure 13. T-wave A-scan data collected from a defect-free chain: amplitude (mV) vs. time (ms).

These signal patterns were also observed in the finite element models. It is evident from the work here that only in the 30–40 and 70–80 kHz bands were the signals optimised. From the modelling, this appears to be a function of the ring spacing.

3.2.3. Conclusion

The propagation of GUW around mooring chains is extremely complex and the modelling and experiments reported here go only part of the way to explaining it. Nevertheless, T-wave propagation was proven to be sensitive to the large defects despite there being more wave modes than are present in LRUT of pipes. L-wave propagation along bars is extremely complex and only if signal processing methods can be developed to differentiate the modes might L-waves be considered for testing chains.

Also, the best resolution was obtained within certain frequency bands, evident in both the numerical modelling and the experiments.

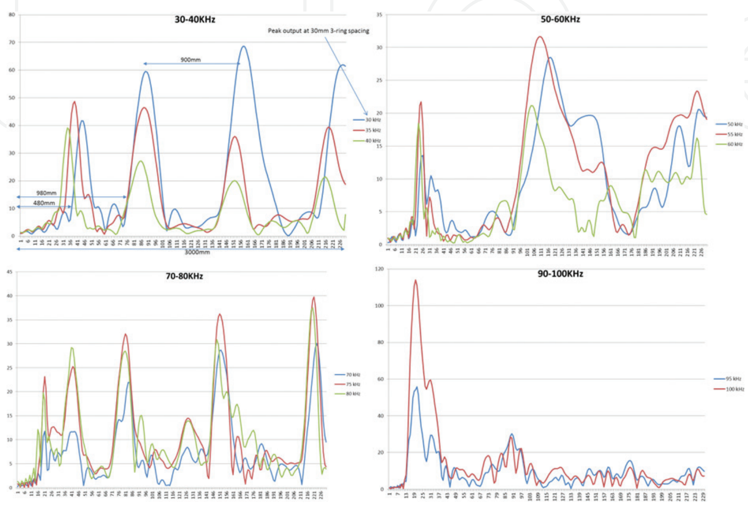

Figure 14. A-scans at different frequencies from 30 to 100 kHz: amplitude (mV) vs. time (ms).

4. Acoustic emission approach

Structural integrity approaches have strongly recommended monitoring mooring chains *in situ* during operation to verify mooring integrity. To more accurately assess the operational condition of in-service mooring chains, it is beneficial to investigate the next-generation of monitoring technologies and their ability to detect flaws and corrosion prior to critical failure. One promising monitoring tool for providing early warning of flaws is acoustic emission testing (AET), which has been used to successfully detect cracks in marine structures during operation.

Acoustic emissions are elastic waves that are spontaneously released by a material undergoing deformation. Acoustic emissions, or so-called 'hits' or events are the stress waves produced by the sudden internal stress redistribution of a material caused by changes in the internal structure. The stress can be hydrostatic, pneumatic, thermal or bending. Possible causes of the internal structure changes are crack initiation and growth, crack opening and closure, dislocation movements. Materials emit ultrasound when they are stressed and fail on a microscopic scale [11].

The optimum AE parameters must be estimated for each application. The appropriate selection and installation of the AE sensors is crucial for a precise data collection strategy. The data must be processed to determine crack initiation and growth and to discriminate irrelevant information.

Acoustic emissions are used to detect defects in structures both in service and during manufacture. The technique can also be used to monitor defect growth during mechanical test in the laboratory. It is an ideal method for examining the behaviour of materials deforming under load.

The difference between an AE technique and other NDT methods is the former detects active defects inside the material, while other the latter attempt to detect passive and active defects. Furthermore, AE needs only the input of one or more relatively small sensors on the surface of the structure or specimen being examined, so that the structure or specimen can be subjected to the in-service or laboratory operation, while the AE system continuously monitors the progressive damage.

The disadvantage of AE is that AE systems can only estimate qualitatively the extent of damage or size of defect. So, other NDT methods are still needed to do more exhaustive examination and provide quantitative results. Conventional ultrasonic evaluation is often used to evaluate AE indications.

4.1. Finite element modelling

Again FEA has been used to analyse the AE wave propagation along the structure. As described in section 3.1, the model is linear elastic and assumed the following material properties for carbon steel.

- Young's modulus = 207 GPa
- Poisson's ratio = 0.3
- Density = 7830 kg/m^3.

http://dx.doi.org/10.5772/intechopen.68386

A chain link of diameter 76 mm was used in the analysis.

A static analysis was run with a pressure of 1000 Pa to find the equilibrium state. The force was applied on the region shown **Figure 15a** which gave the result shown in **Figure 15b**

A dynamic model was created with the same geometry and same pressure applied, but with a crack inserted at the position indicated in **Figure 16**. The shape was a segment of the circle, with a maximum depth of 10 mm. The position was at the inner side of the join between the curved section and straight section of the chain link.

Stresses from the static model were applied to the dynamic model as the initial conditions.

Two AE sensors were modelled in the dynamic model. Each was 10 mm long, 29 mm around the circumference and positioned at 146.4 mm along from the plane of the crack. They were positioned one at the top of the model (Sensor 1) and one at the bottom (Sensor 2) as shown in **Figure 17**. The outputs were requested in the local cylindrical coordinate system (r, θ, z).

4.1.1. Modelling results

The dynamic model was solved in Abaqus for a simulated time of 0.5 ms. The crack opening can be observed in **Figure 18**.

The AE wave propagation and the displacement generated by the simulated crack growing can be observed in **Figure 19**. This relates directly with the elastic waves released at the crack tip.

The (r, θ, z) components of the displacements at each sensor location were recorded. **Figure 20** shows the displacement amplitude at both sensors location. The time of arrival (ToA) at each sensor can be observed. Calculating the value of the ToA, parameters such as the wave velocity or the location and time of occurrence can be estimated.

4.2. Methodology and experiments on chain links

Following the FEA analysis, a mooring chain link was monitored using AE in a simulated seawater tank tensile test rig. The rig is able to apply variable tension to a single link. A notch was initially introduced into the chain. During the test, a tensile load was applied at the

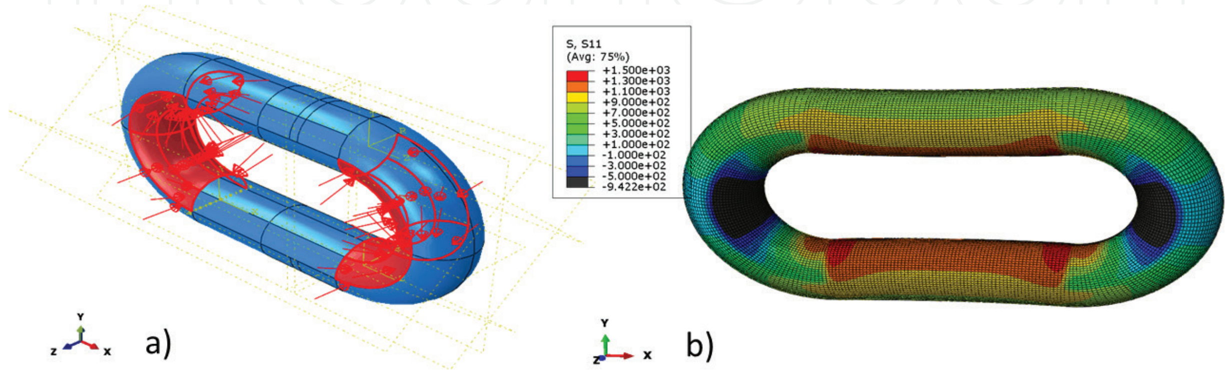

Figure 15. (a) Area were force is applied and (b) distribution of stress along the chain.

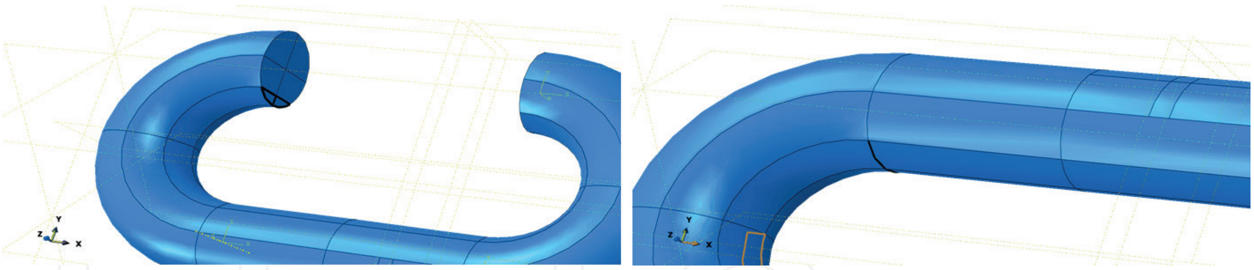

Figure 16. Chain seam model view.

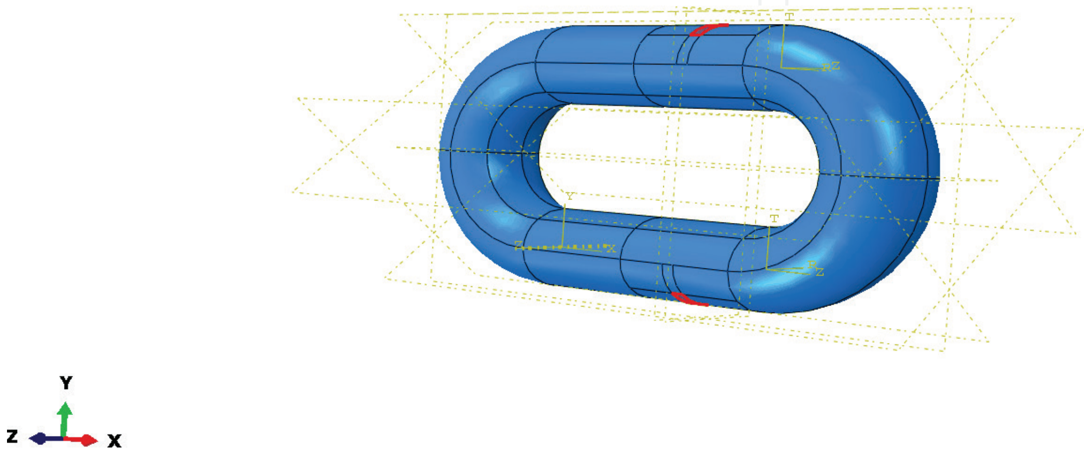

Figure 17. AE sensors location: Sensor 1 top, Sensor 2 bottom.

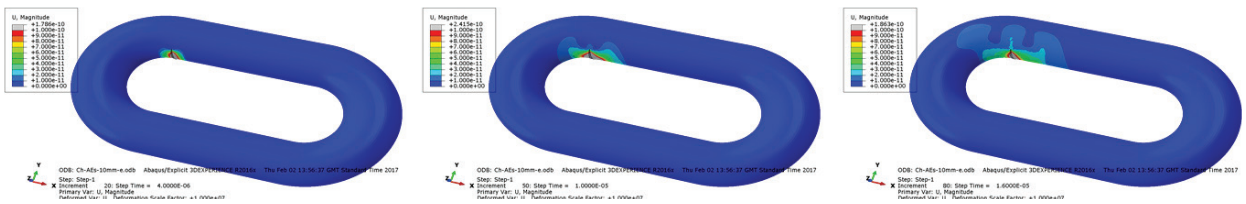

Figure 18. Crack opening model.

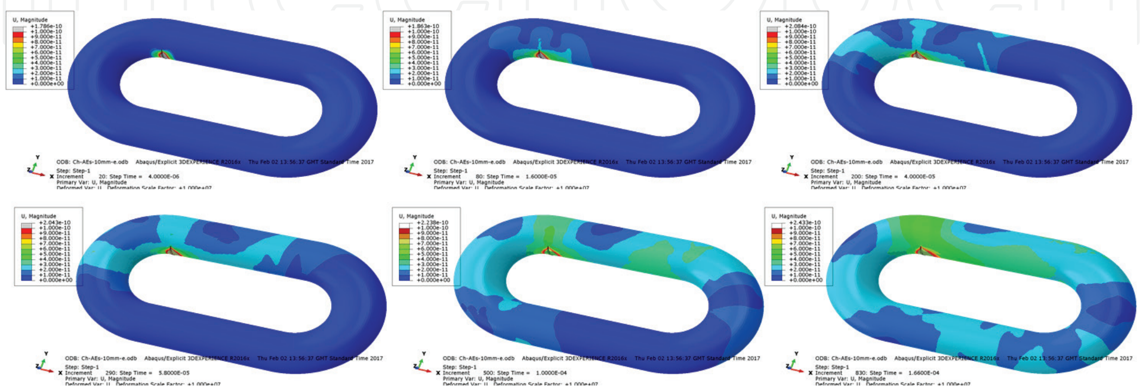

Figure 19. Elastic wave propagation model.

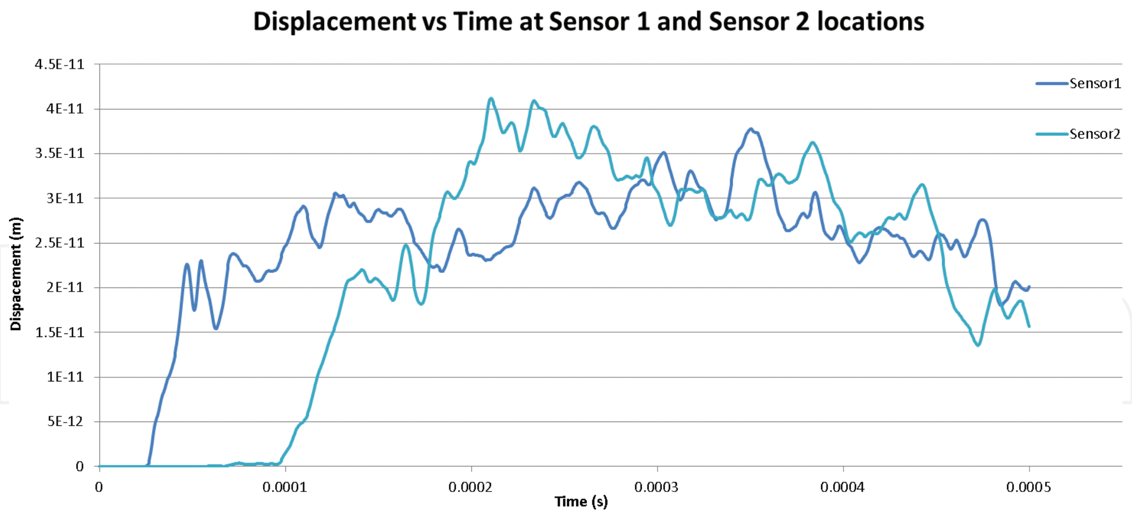

Figure 20. AE waveform for S1 and S2: displacement module vs. time.

connection point of the chain. The location of the sensors, forces and AE sensors can be seen in **Figure 21**.

4.2.1. Acoustic emission equipment and specifications

An AE system is a multi-channel data acquisition tool consisting of parallel measurement channels and system front-end software running on an external computer. A measurement channel consists of an AE sensor, AE preamplifier and one channel of an AE signal processor card.

The tensile test rig was instrumented with three AE sensors to record the AE data during the full test. Two AE sensors (150 kHz resonance frequency) were mounted with a magnetic holder on the tank frame to serve as 'guard' sensors in order to filter external environmental noise. The principal sensor used to detect the AE activities was submerged inside the seawater mounted using a magnetic holder. This was an AE sensor with an integrated preamplifier gain of 34 dB. Its resonance frequency was 150 kHz and it had an operating range of 90–450 kHz. It was of a design suitable for wet environments and on-site monitoring of underwater

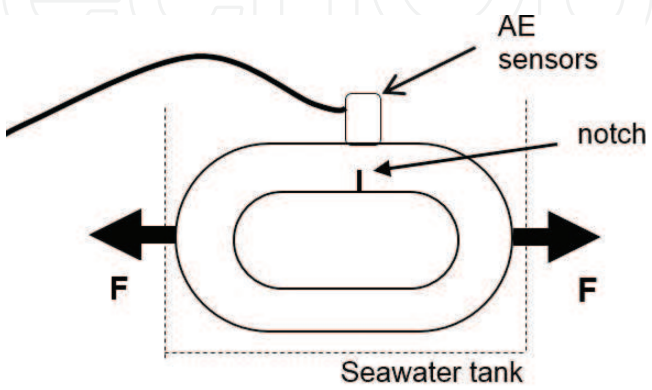

Figure 21. Chain set up under load with induced notch.

installations. The sensor was operated in a passive mode during the whole loading process to detect crack initiation and crack growth.

4.2.2. Experimental results

The laboratory trials were divided in two parts: the first part lasting for 75 hours to calibrate the set-up. In the second part, the system ran continuously for 285 hours to validate the long-term inspection capability. During these two tests, the load applied on the chain was kept constant at 8 MN.

One AE feature that proved to successfully represent crack initiation and propagation is energy. During the experimental test, cumulative energy was continuously calculated and recorded. From the calibration test, the set-up was validated (**Figure 22**).

During the long-term test, AE cumulative energy vs. time illustrated a linear increase in AE activity at first (**Figure 23**); this is followed by a rapid increase of energy when crack was propagating at a large scale.

4.2.3. Conclusion

AE graphs of cumulative energy vs. time show that the mooring chain crack propagation process was captured. The results can be considered as a characteristic curve of crack growth status over time.

Through both the calibration test and long-term test, the ability of the technique to detect and process AE events in real time has been proved. Other AE signal features including duration, peak amplitude together with cumulative energy should be analysed to evaluate the crack growth process.

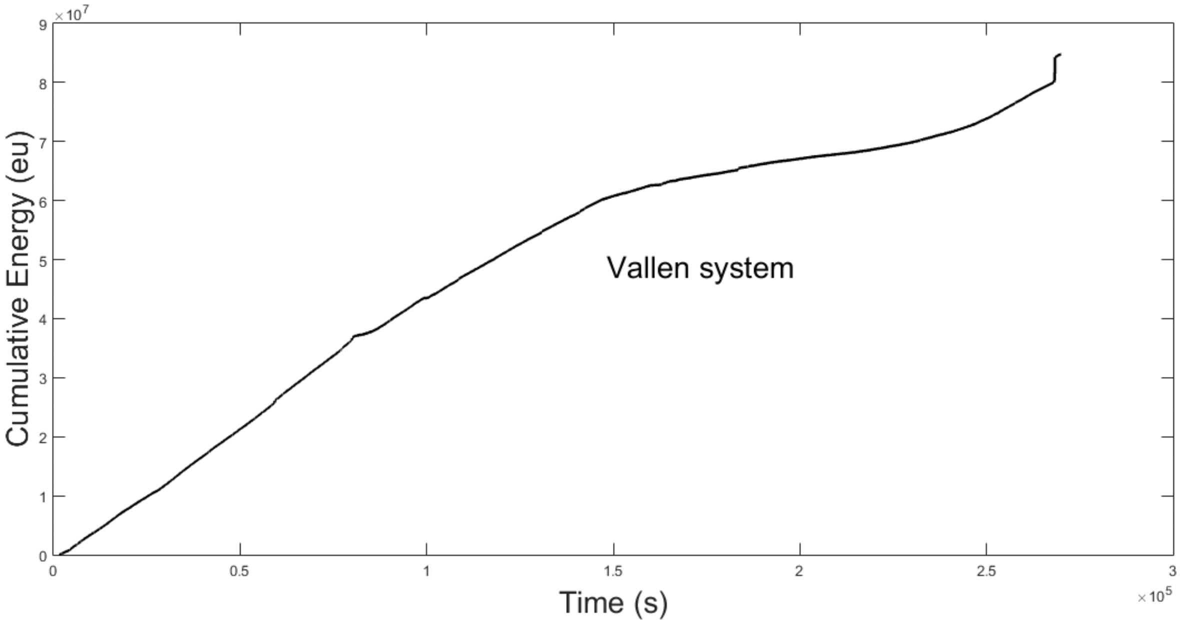

Figure 22. Cumulative energy vs. time (calibration test, 75 h).

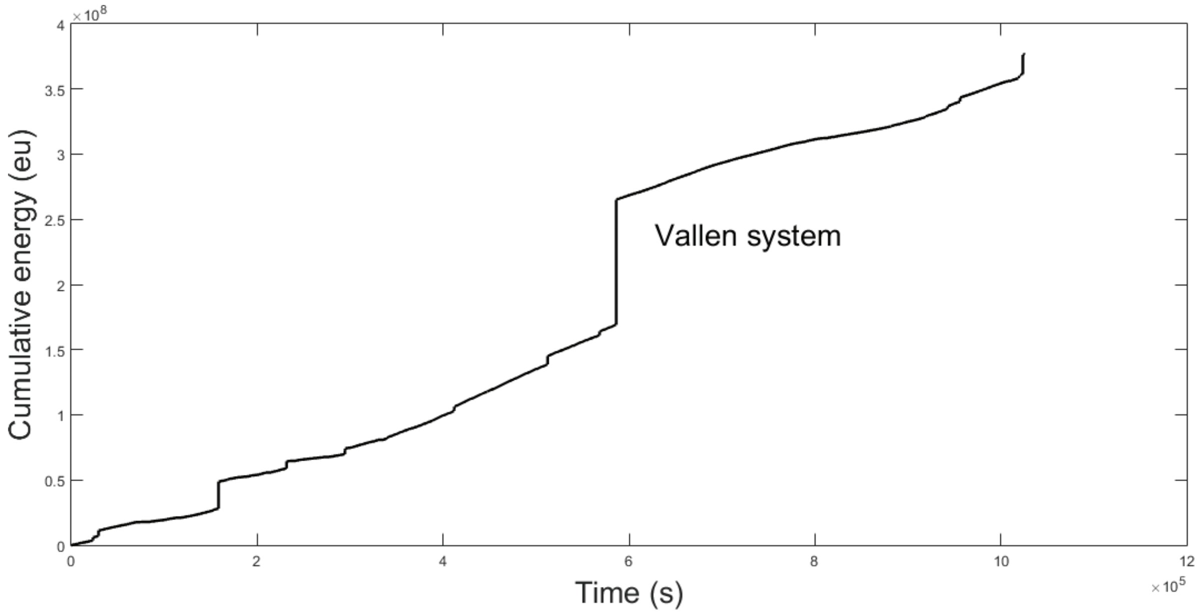

Figure 23. Cumulative energy vs. time (laboratory test, 285 h).

5. Final discussion

Due to the increasing demand of structural retrofit into conventional inspection strategies, SHM is of interest to an extensive range of industries. GUW and AE are non-destructive monitoring techniques which are widely employed at present. The output of its application will be comprehensive, real-time assessment of the structural condition of industrial assets.

The primary goal of this study was to investigate the applicability of GUW and AE approaches for crack initiation, location and propagation on a mooring chain. Modelling work and experimental testing have shown indication of the active damaged regions.

Because of the inherent uncertainties present in any SHM technique, the described technologies should be applied as part of a full mooring chain structural integrity assessment. Recent developments in internet infrastructure and connectivity for monitoring and sensing present an opportunity to overcome the limitations of AE and GUW testing for continuous monitoring. In addition to the continuous data output, a risk-based integrity management strategy may also include, where available, data from periodic inspections, numerical modelling showing stress distributions or crack propagation, historic and current operations.

Author details

Ángela Angulo, Graham Edwards, Slim Soua and Tat-Hean Gan*

*Address all correspondence to: tat-hean.gan@twi.co.uk

TWI Ltd, Integrity management Group, Granta Park, Great Abington, Cambridge, United Kingdom

References

[1] EU Commission Database on Number of FPS Drilling in European Waters. October 2010

[2] Applicable to the DnV Standard, International NDT (EN473 or ISO 9712)

[3] Lloyds Rules and Regulations for the Classification of a Floating Offshore Installation at a Fixed Location. Published by Lloyd's Register Group Limited, London, United Kingdom. Parts 1 to 11, 2013

[4] Floating production system. JIP FPS mooring integrity. Prepared by Noble Denton Europe Limited for the Health and Safety Executive, Norwich, United Kingdom, 2006

[5] International Energy Outlook 2016. Chapter 1. World energy demand and economic outlook. U.S. Energy Information Administration's, DOE/EIA-0484, May 11, 2016

[6] Richard Youngs. Energy Security, Europe's New Foreign Policy Challenge. Taylor & Francis, Abingdon, United Kindom, January 2009 Jan 28, 2009

[7] Farleyefndt M. Guidelines on the overall NDT quality system in Europe. In 17th World Conference on Non-destructive Testing, Shanghai, China; 2008

[8] Raj B. Non-Destructive Testing and Evaluation: Overview, Encyclopaedia of Materials: Science and Technology. India: Indira Gandhi Centre for Atomic Research; 2011. pp.6177-6184

[9] Larsen and Fylling, SeaTek Corp, Potts, Texas United States. 1982, 1981, 1993.

[10] Sanderson, R. M., & Smith, S. D.. The application of finite element modelling to guided wave testing systems. In D. O. Thompson, D. E. Chimenti, C. Nessa, S. Kallsen, & L. Poore, AIP Conference Proceedings (Vol. 657, No. 1, pp. 256–263). March 2003

[11] Huang, M, et al. Using acoustic emission in fatigue and fracture materials research. JOM. 1998;**50**:(11): 1-14

[12] Catton. Long range ultrasonic guided waves for the quantitative inspection of pipelines. Eng.D. thesis, School of Engineering and Design, Brunel University, London, England, 2009, pp. 2–4.